

# 3-D inversion of induced polarization data in wavelet domain

Yaping Zhu\* and Yaoguo Li, Department of Geophysics, Colorado School of Mines

## Summary

We develop an algorithm of constrained inversion of IP data for recovering 3D chargeability in the wavelet domain. The inversion is regularized directly by using a scale dependent objective function, while positivity is achieved through conditions imposed on the multiresolution representation of the chargeability so that nearly positive solutions are obtained. Accomplishing the inversion entirely in the wavelet domain leads to an algorithm more efficient than those in the space domain. We illustrate the algorithm using a synthetic 3-D data set here and will also demonstrate its practical application to large field data sets.

## Introduction

Inferring mineral deposits based on induced polarization (IP) data has evolved from qualitative interpretation of pseudosections to inversion of 2-D and 3-D IP data. A number of inversion algorithms exist and they are primarily based on Seigel's (1959) phenomenological model of IP effect. This representation states that the presence of chargeability effectively reduces the conductivity of the medium and the resulting potential is governed by the same equation as in DC resistivity:

$$\nabla \cdot (\sigma(1 - \eta)\nabla\phi_\eta) = -\delta(\mathbf{r} - \mathbf{r}_s), \quad (1)$$

where  $\sigma$  is the conductivity as a function of position  $\mathbf{r}$  in three dimensions beneath the earth's surface,  $\mathbf{r}_s$  is the location of the source,  $\eta$  is the chargeability, and  $\phi_\eta$  is the total potential. By assuming the chargeability to be small and the IP data unaffected by EM coupling, this representation yields the linearized equation

$$\sum_{k=1}^{n_m} G_{ik}\eta_k = \eta_{ai}, \quad 1 \leq i \leq n_d, \quad (2)$$

where  $\eta_k$  denotes the chargeability of the  $k$ th region in the subsurface,  $\eta_{ai}$  is the  $i$ th apparent chargeability.  $n_d$  and  $n_m$  are, respectively, the number of the data measurements and the number of the model cells after discretization of the subsurface region.

One challenge encountered in conventional IP inversion is the computational cost required in the iterative inversion algorithms. Wavelet transform has been introduced as a powerful tool to speed up the inversion. Due to the localized property of a wavelet, a sparse representation of the sensitivity matrix is obtained in the wavelet domain via removing wavelet coefficients whose magnitudes are below a specified threshold. Hence, the forward problem is solved using a compressed sensitivity matrix. A fast constrained inversion using wavelet transform was discussed

by Li and Oldenburg (2000), where forward modeling is performed in the wavelet domain while the inversion is carried out in the spatial domain, i.e., the objective function and its gradients are expressed in terms of the model in the spatial domain. Such a methodology only partially utilizes the advantages offered by wavelet transforms. In particular, it requires transforming the model back and forth between the two domains during the inversion and imposing positivity in the space domain.

We propose to carry out the constrained inversion entirely in the wavelet domain by utilizing a model objective function based on the wavelet coefficients of the chargeability and imposing bound constraints on the chargeability through its multiresolution representation. The algorithm allows one to construct a smooth, nearly-positive chargeability model with much less computational cost.

## Formulating the inversion

Consider the linear system (2), rewritten as  $\mathbf{G}\eta = \mathbf{d}$ . Wavelet transform can be applied to both the chargeability model and each row of the sensitivity matrix:  $\tilde{\mathbf{G}}\tilde{\mathbf{m}} = \mathbf{d}$ , where  $\tilde{\mathbf{G}} = \mathbf{G}\mathcal{W}^T$ ,  $\tilde{\mathbf{m}} = \mathcal{W}\eta$ , and  $\mathcal{W}$  represents a 3D wavelet transform, which transforms the model and each row of the matrix into the wavelet domain. We remark that the chargeability model can be discretized uniformly and thereby allows the implementation of standard wavelet transform. The IP data are usually irregularly located and they are not easily wavelet-transformed. For this reason, we focus on transforming the model only.

The wavelet transform based on the pyramid algorithm (Mallat, 1989) produces a series of wavelet coefficients for a signal at various scales  $j=0, \dots, J$ , where  $j=0$  denotes the finest scale and  $J$  the coarsest scale. The wavelet coefficients consist of (1) the smooth-part coefficients,  $v_{j,k}$ , which contain information that generally corresponds to various low-frequency representations of the functional, and (2) the detailed-part coefficients,  $w_{j,k}$ , which generally depict the details of the function at various scales, where  $1 \leq k \leq n/2^j$  and  $n$  is the length of the signal.

The transformed matrix  $\tilde{\mathbf{G}}$  is first made sparse by applying thresholding. Subsequent forward modeling in the wavelet domain is achieved by a multiplication between the sparse matrix and the transformed model vector. Since only significant coefficients with values above the threshold in  $\tilde{\mathbf{G}}$  are stored and used in the computation, this yields the desired reduction in both memory requirement and CPU time.

The objective function consists of a data misfit term  $\Psi_d$  and model objective function  $\Psi_m$ :

$$\Psi = \Psi_d + \mu\Psi_m, \quad (3)$$

### 3-D inversion of induced polarization data in wavelet domain

where  $\mu$  is the regularization parameter determining the relative importance of the data misfit and the model objective function.

Since the data are not transformed into the wavelet domain, the data misfit term has the same form as that in the space domain,

$$\Psi_d = \|\mathbf{W}_d(\mathbf{d}^{\text{pre}} - \mathbf{d}^{\text{obs}})\|^2, \quad (4)$$

where  $\mathbf{d}^{\text{pre}}$  and  $\mathbf{d}^{\text{obs}}$  are predicted and observed data, respectively.  $\mathbf{W}_d$  is a diagonal weighting matrix whose elements can be the inverse of the standard deviation of the estimated error of each datum,  $\mathbf{W}_d = \text{diag}\{1/\epsilon_1, \dots, 1/\epsilon_{n_d}\}$ .

In the wavelet domain, the model objective function is expressed in terms of the wavelet coefficients of the model,

$$\Psi_{\tilde{\mathbf{m}}} = \|\mathbf{W}_{\tilde{\mathbf{m}}}(\tilde{\mathbf{m}} - \tilde{\mathbf{m}}_0)\|^2, \quad (5)$$

where  $\tilde{\mathbf{m}}$  and  $\tilde{\mathbf{m}}_0$  are, respectively, the wavelet representation of the unknown model and that of the reference model. The weighting matrix  $\mathbf{W}_{\tilde{\mathbf{m}}}$  is diagonal and its elements  $W_{\tilde{\mathbf{m}},k}$  are constructed to compensate the decay of the variance of the model wavelet coefficients across scales. For example,  $W_{\tilde{\mathbf{m}},k} = 2^{\beta \cdot \sqrt{j_x^2 + j_y^2 + j_z^2}}$  indicates a scale-dependent weighting, where  $\beta$  determines the decay rate of the variance across scales,  $j_x$ ,  $j_y$ , and  $j_z$  denote the scale indices in different spatial directions. The model weighting matrix constructed in this way yields a smooth model that is similar to those obtained using a smooth regularizer in the space domain. Because  $\beta$  can be adjusted for different scales, such a model objective function provides flexibility in constructing models with different smoothness.

To complete the inversion algorithm, we also need to apply bound constraints on the chargeability values to guarantee the feasibility of the recovered chargeability model:

$$m_{\perp} \leq \mathbf{m} \leq m_{\top}, \quad (6)$$

where  $m_{\perp}$  and  $m_{\top}$  denote, respectively, the lower and upper bound of the model values. Such straightforward inequality constraints become much more complicated in the wavelet domain since each model value in the space domain is affected by a large number of wavelet coefficients:

$$m_{\perp} \leq \mathcal{W}^T \tilde{\mathbf{m}} \leq m_{\perp}. \quad (7)$$

Straightforward implementation of the above condition necessitates the transform back to the space domain during the inversion, which requires extra computational cost. Hence, the second part of this study is devoted to an efficient implementation of the bound constraints in the wavelet domain.

#### Near-positivity constraint

A constraint frequently used in IP inversion is that the chargeability is positive, which is easily represented in the

space domain. In the wavelet domain, however, a bound constraint (with positivity as a special case) requires imposing conditions in equation (7) and necessitates the transform back to the space domain. To avoid such difficulties, we represent the bound constraints at various coarse scales in the wavelet domain so that a high degree of approximation to the bound constraint is achieved with little computational overhead. The result is a nearly positive chargeability model that is sufficient for practical applications.

The near-positivity constraints are represented in a cascade fashion. At scale  $j = 0$ , the chargeability values are positive since they are represented in the physical domain. When the chargeability model is transformed into the wavelet domain, its representation at an intermediate scale  $j$  ( $1 \leq j \leq J$ ) is generally positive because of the positivity of the scaling filters in the wavelet transform, i.e.,

$$\tilde{m}_{j,k} \geq 0, \quad 1 \leq j \leq J, \quad 1 \leq k \leq n/2^j, \quad (8)$$

where  $n$  denotes the length of the signal, which is a power of two. Such a behavior can be considered analogous to low-frequency trend of the positive signal after low-pass filtering. Positivity at scale  $J$  is comparable to making DC components of the chargeability positive.

Although strictly-positive chargeability is not guaranteed, the constraints on the representations at various scales make the chargeability nearly positive. When a Haar wavelet is used, positivity in the spatial domain is equivalent to the requirement that the multiresolution representation across all scales  $0 \sim J$  are positive. For other types of wavelets such as the Daubechies-4 wavelet (Daubechies, 1992), the positivity cannot be achieved rigorously by only constraining coarse-scale coefficients. However, it usually provides a nearly-positive solution of the recovered model.

For bound constraints, the cascade representation is given as

$$\tilde{m}_{\perp,j,k} \leq \tilde{m}_{j,k} \leq \tilde{m}_{\top,j,k}, \quad 1 \leq j \leq J, \quad 1 \leq k \leq n/2^j, \quad (9)$$

where  $\tilde{m}_{\perp,j,k}$  and  $\tilde{m}_{\top,j,k}$  denote, respectively, the multiresolution representation of the lower and upper bounds of the model.

The cascade positivity constraint is achieved by applying an incomplete wavelet transform which transforms the wavelet coefficients back to an intermediate scale depending on which scale is selected to represent the constraint. To incorporate the constraints into the objective function, we adopt a logarithmic barrier method in which the bound constraints are represented as a logarithmic barrier term:

$$\Psi = \Psi_d + \mu \Psi_m - 2\lambda \sum_{j,k} \left( \ln \frac{\tilde{m}_{j,k} - \tilde{m}_{\perp,j,k}}{\tilde{m}_{\top,j,k} - \tilde{m}_{\perp,j,k}} + \ln \frac{\tilde{m}_{\top,j,k} - \tilde{m}_{j,k}}{\tilde{m}_{\top,j,k} - \tilde{m}_{\perp,j,k}} \right), \quad (10)$$

where  $\lambda$  is the barrier parameter. The minimization starts with a feasible initial model that satisfies the constraints.

### 3-D inversion of induced polarization data in wavelet domain

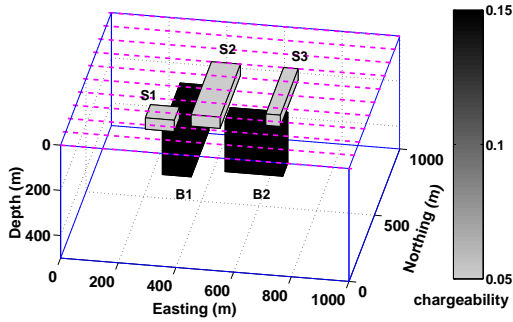


Fig. 1: 3-D perspective view of the five-prism chargeability model. Three prisms near the surface are denoted as S1–S3 with chargeability 5%. The other two prisms at the deeper depth are denoted as B1 and B2 with chargeability 15%. Eleven easting-westing survey lines are used spaced 100-m apart, as denoted with dashed lines.

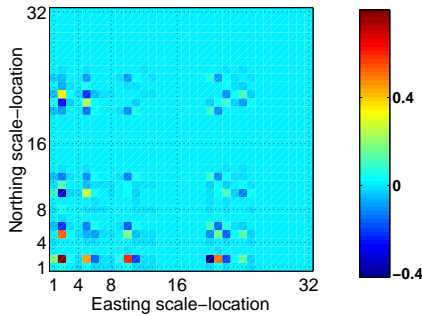


Fig. 2: A horizontal slice of the chargeability model in the wavelet domain. The Daubechies-4 wavelet is used. Dashed lines are used to demarcate blocks of different scales.

A large positive number is set as the initial value of  $\lambda$ . The objective function (10) is then minimized for a sequence of  $\lambda$  with decreasing values. At each iteration, we obtain feasible solution that satisfies the condition (8) or (9). This solution then serves as the initial model for the next iteration. As  $\lambda$  reduces to a value close to zero, the recovered model converges to an optimal solution for which the constraint condition is met.

#### Numerical example

We now illustrate the inversion algorithm using a synthetic example. The data are generated from a model consisting of five individual prisms with anomalous conductivity and chargeability embedded in a uniform background of zero chargeability (Figure 1). Three surface prisms simulate near-surface distortions, and two buried prisms simulate deeper targets. The central region of the model is discretized into a uniform mesh made up of  $20 \times 20 \times 20$  cells, with the size of  $50 \text{ m} \times 50 \text{ m} \times 25 \text{ m}$ . Here we adopt a right-handed Cartesian coordinate system with  $x$  positive north,  $y$  positive east, and  $z$  positive down. After the model is padded with zeros, the total number of cells is  $32 \times 32 \times 32$ . A 3-D separable wavelet

transform is then applied to the model with the scale range of  $(0,0,0)$ – $(3,3,3)$ . Figure 2 shows a horizontal slice of the wavelet representation of the model with 64 blocks resulting from the 3-D transformation: in each direction the wavelet transform produces four parts of coefficients,  $v_{3,k}$ ,  $w_{3,k}$ ,  $w_{2,k}$ , and  $w_{1,k}$ , where  $k$  is the scale-location of the coefficients at the corresponding scales.

Apparent chargeability data are simulated for a pole-dipole array with  $a=50 \text{ m}$  and  $n=1\sim 6$ . Eleven survey lines are acquired that are spaced 100-m apart and oriented in east-west direction (Figure 1). The number of data is 1089. These were then contaminated by pseudo-random Gaussian noise. For the IP inversion, we assume the conductivity model has been recovered from a prior inversion of the accompanying DC resistivity data.

We first invert the data without constraint on the chargeability. The initial chargeability model is set to zero. After obtaining the inverted wavelet coefficients in the wavelet domain, we carry out the inverse wavelet transform to obtain the recovered chargeability. Inversion without constraint generates a model that resembles the near-surface structure (Figure 3a). A large portion of the recovered model, however, shows negative chargeability that is unreasonable.

Next, we perform the inversion with positivity constraints at scale  $(1, 1, 1)$ . At this stage, the initial model is the one recovered from the unconstrained optimization and is then adjusted to form a feasible model, i.e., we raise negative parts of the model to make the overall chargeability positive. The inversion starts with the feasible model and produces the recovered model as shown in Figure 3b. Incorporating constraints at scale  $(1,1,1)$  improves the model by eliminating some negative values in the recovered model. Since the constraints are not applied to the full scale range, the model is still not entirely positive.

In comparison to the two inversions discussed above, we apply the inversion with constraints at scale  $(0,0,0)$ , i.e., the positivity constraints is formulated in the spatial domain, as performed in the conventional inversions. The recovered model, shown in Figure 3c, then becomes positive. We note that the recovered nearly-positive model in Figure 3b is virtually indistinguishable from that shown in Figure 3c. The former, of course, requires much less computational cost to obtain. Our experience shows that for larger inversion problem, scale  $j = 1$  or 2 are good choices of scale at which to impose positivity.

#### Discussion

We have developed an efficient algorithm for inverting 3D induced polarization data in the wavelet domain. The algorithm first transforms both the sensitivity matrix and the model into the wavelet domain and generates a sparse system by applying wavelet thresholding. We formulate the inverse problem by treating the wavelet coefficients of the chargeability as unknown parameters and utilizing a scale-dependent model objective function. The choice of model objective function is flexible in recovering charge-

### 3-D inversion of induced polarization data in wavelet domain

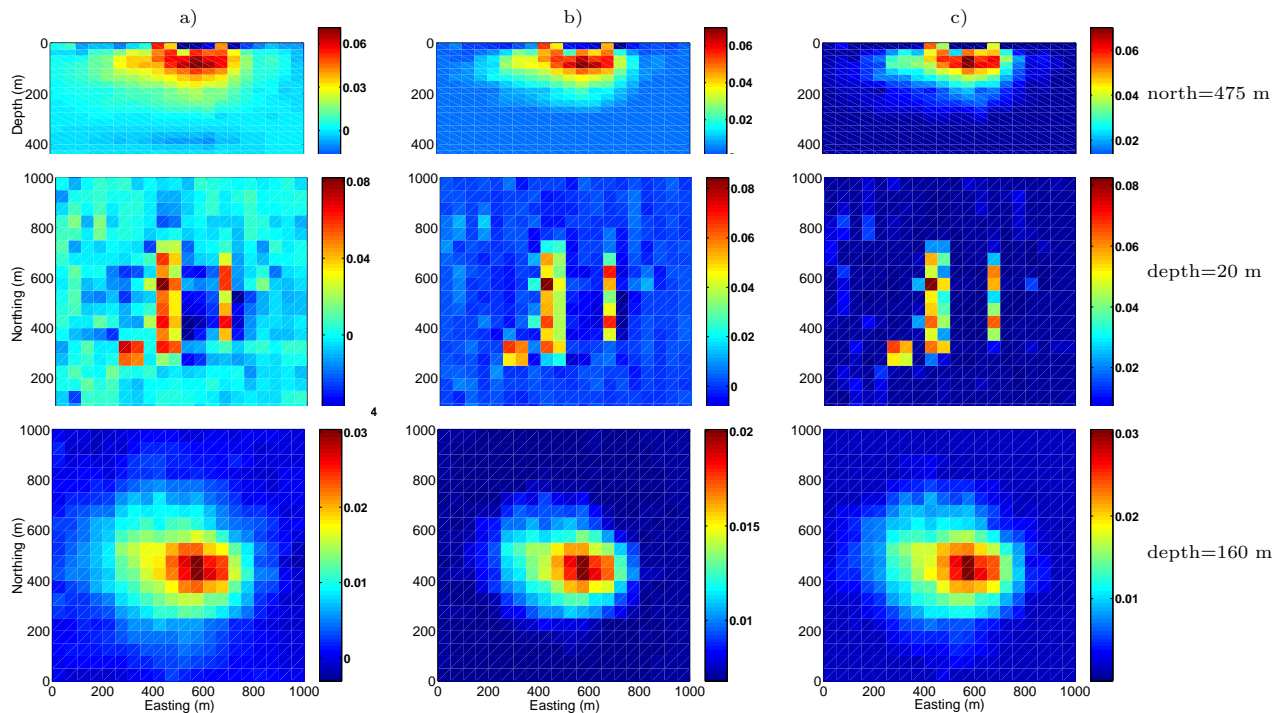


Fig. 3: Chargeability models recovered from a) unconstrained optimization, b) constrained optimization with positivity represented at scale (1, 1, 1), and c) constrained optimization with positivity represented at scale (0, 0, 0). Top: north=475 m; middle: depth=20 m; bottom: depth=160 m. The color scales indicate the recovered chargeability values.

ability models with different smoothness properties with simple adjustment of an exponential parameter.

An important benefit of the algorithm is its computational efficiency. The speed-up of the inversion is achieved primarily from the sparse sensitivity matrix in the wavelet domain, which allows us to solve large problems more rapidly. In addition, we have developed an approximate approach for imposing space-domain bound constraints directly in the wavelet domain with minimal computational overhead. The result is a nearly-positive chargeability model that is virtually identical as a strictly positive model but with less computational cost.

The performance of the near-positivity constraints is also influenced by the choice of wavelets. When a Haar wavelet is used, requiring smooth-part coefficients to be positive while setting their accompanying detailed-part coefficients to zeros always produces strictly positive solution. Other types of wavelets such as Daubechies-4 wavelet yield only near-positive solutions. In general, since the constraints are implemented by using incomplete wavelet transform, there is a trade-off between the computational cost and how close the solution is to a strictly positive one. This tradeoff can be adjusted by users depending on the intended use of the inversion result. For example, earlier, trial inversion can be carried out with loose approximation to the constraints while the final inversion for making an exploration decision can be done with a higher degree of approximation.

### Acknowledgments

This work was jointly supported by the sponsors of the Consortium Project on Seismic Inverse Methods for Complex Structures at the Center for Wave Phenomena and the Gravity and Magnetics Research Consortium at the Colorado School of Mines.

### References

- Daubechies, I., 1992, Ten lectures on wavelets: SIAM, Philadelphia.
- Li, Y., and Oldenburg, D. W., 2000, 3-D inversion of induced polarization data: *Geophysics*, **65**, 1931–1945.
- Mallat, S., 1989, Multifrequency channel decompositions of images and wavelet models: *IEEE Transactions on Acoustics, Speech and Signal Processing*, **37**, 2091–2110.
- Seigel, H. O., 1959, Mathematical formulation and type curves for induced polarization: *Geophysics*, **24**, 547–565.